

Sub-micromolar affinity of *Escherichia coli* NikR for Ni(II)

Rutger E.M. Diederix, Caroline Fauquant, Agnès Rodrigue, Marie-Andrée Mandrand-Berthelot, and Isabelle Michaud-Soret

I. When NikR is in excess over Ni(II), no aggregates are present.

Dynamic light scattering experiments were performed with wt NikR in the absence and presence of various Ni(II) concentrations (Figure S1). NikR was 20 μ M (20mM Hepes pH 8, 0.1 M NaCl). The experiments were recorded using a Zetasizer nanoS from Malvern Instruments using a 50 μ L quartz cuvette at 293K. NikR was allowed to incubate for 20 min with NiSO₄ prior to the measurements. When NikR is in 10-fold or higher excess over Ni(II), no aggregation is observable (Fig. S1A). At higher concentration of Ni(II), aggregation is observed (Fig. S1B), but this disappears with time. It can be concluded that under the conditions of the UV/vis titrations as well as the Ni(II) binding kinetics experiments, Ni(II)-induced NikR aggregation does not play a role.

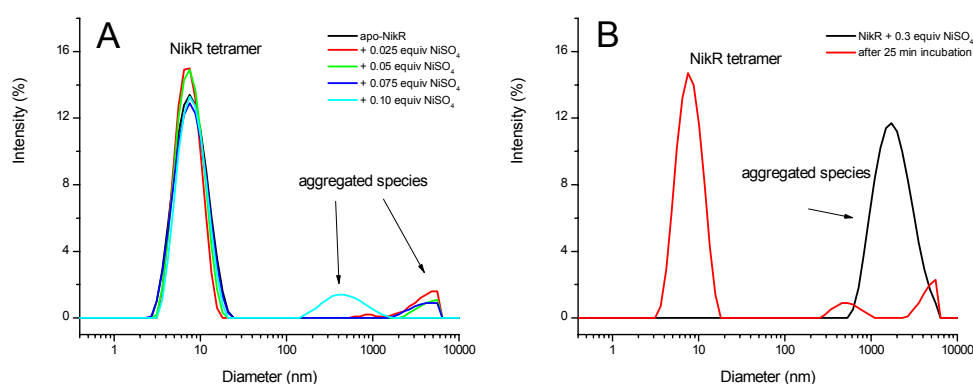


Figure S1. Dynamic light scattering of NikR in the absence and presence of increasing Ni(II). A) A titration with Ni(II) up to 0.1 equivalent. Tetrameric NikR, corresponding to the species with diameter ~7.5 nm, is the major species present, representing 100, 91, 95, 95 and 87 respectively, of the total intensities of NikR with increasing Ni(II) concentration. B) NikR with 0.3 equivalent Ni(II). Initially all the protein is present in the form of large aggregates (diameter 2 μ m), but this is reversed with time. After 25 min, almost all the protein is tetrameric again.

II. Determining the K_D with $[NikR] \gg [Ni(II)]$ by UV/vis titrations.

Ni(II) titrations were performed with Q2E NikR in 20 mM Hepes pH 8.0, 0.1 M NaCl, 293 K. Q2E NikR concentrations used were 0.6, 0.94, 1.1, 1.5, 2, 3, 3.1, 6, 12.6, 60, 215, and 860 μ M. Lower protein concentrations were not used because of diminished reliability of absorbance values. The mixtures were allowed to equilibrate for at least 30 min after addition of the NiSO₄ before UV/vis spectra were acquired. UV/vis spectra were acquired using a Hewlett-Packard 8453 diode array spectrophotometer, thermostated at 293 K. Depending on the protein concentration, cuvettes with optical path lengths of 0.1, 1 and 10 cm were used. The ‘linear absorbance increase’ is defined as the linear dependence of absorbance at 302 nm on [NiSO₄] between 0 and 0.1 equivalents. NikR is a tetrameric protein, with 4 His₃Cys sites capable of Ni(II)-binding with high affinity (HA sites). No co-operativity

Supplementary Material (ESI) for Chemical Communications

This journal is (c) The Royal Society of Chemistry 2008

between the sites is present, as evidenced by linear Ni(II) binding curves [1]. If $[Ni(II)]$ remains less than 10% of $[NikR]$, we can consider independent binding of Ni(II) to each of the sites representing the macroscopic dissociation constant. Binding of Ni(II) to the His₃Cys binding sites becomes partial when the concentration of these sites become close or inferior to the K_D . This fractional binding of Ni(II) has a hyperbolic dependence on $[NikR]$. This is justified below for the simple binding equilibrium $Ni(II) + NikR \rightleftharpoons Ni\text{-}NikR$:

$$K_D = \frac{[NikR]_{\text{free}} \cdot [Ni(II)]_{\text{free}}}{[Ni - NikR]} \quad (1)$$

When $[NikR]_{\text{tot}} \gg [Ni(II)]_{\text{tot}}$ it follows that:

$$[NikR]_{\text{free}} \approx [NikR]_{\text{tot}} \quad (2)$$

and

$$[Ni(II)]_{\text{free}} = [Ni(II)]_{\text{tot}} - [Ni\text{-}NikR] \quad (3)$$

Substitution of eq. 2 and eq. 3 in eq. 1, and subsequent rearrangement gives:

$$[Ni - NikR] = \frac{[Ni(II)]_{\text{tot}} \cdot [NikR]_{\text{tot}}}{(K_D + [NikR]_{\text{tot}})} \quad (3)$$

The absorbance increase at 302 nm with increasing Ni(II) concentration corresponds to the formation of Ni-NikR. The ratio $[Ni\text{-}NikR]/[Ni(II)]_{\text{tot}}$ is the fractional binding of Ni(II), is equal to the ratio of the linear increase in absorbance and the extinction coefficient ϵ_{302} :

$$\frac{[Ni - NikR]}{[Ni(II)]_{\text{tot}}} = \frac{\text{linear absorbance increase}}{\epsilon_{302}} \quad (4)$$

Substitution into eq. 3 and subsequent rearrangement gives the hyperbolic relationship (eq. 5):

$$\text{linear absorbance increase} = \epsilon_{302} \cdot \frac{[NikR]_{\text{tot}}}{(K_D + [NikR]_{\text{tot}})} \quad (5)$$

III. The filter binding assays and fitting of the data.

The filter binding assay data were analyzed using DynaFit [2]. We assumed independent binding to two categories of binding sites, each with a different affinity for Ni(II) [1]. The HA site is considered one category, while all other sites that are rapidly depleted by EDTA are considered the second category (low affinity, LA sites). Only one HA site is present per NikR monomer, and, for sake of simplicity, we assumed only 3 LA sites, each with equal affinity for Ni(II). These represent the entirety of sites present on NikR capable of binding Ni(II). It was assumed that wt and Q2E NikR possess both HA and LA sites; EDTA-washed wt and Q2E NikR only HA sites, and Q2E/H89N NikR only LA sites. The data were fit independently and the resulting K_D 's averaged. The K_D of the LA binding site was first determined using the data for Q2E/H89N NikR and this value used to fit the data for wt and Q2E NikR.

Supplementary Material (ESI) for Chemical Communications

This journal is (c) The Royal Society of Chemistry 2008

IV. Fitting of the Ni(II)-binding kinetics to NikR.

Non-linear least-squares fitting of the stopped-flow traces to a single exponential gives imperfect fits, with clear deviations at the beginning of the reactions (i.e. evidence of a lag-phase). Also, the rate constants derived from this fitting display a hyperbolic dependence on [NikR]. Together, this can be taken as evidence of a mechanism of binding that involves an intermediate species and that the species giving the signal (i.e. absorbs at 302 nm) is the species that follows the intermediate in the reaction sequence [3, 4]. The most simple and likely reaction mechanism is a two-step binding mechanism. From a structural point of view, this is also likely; the HA (His₃Cys) site is situated in the interior of the protein, and the most direct route for Ni(II) ion to the HA site is through a cluster of His residues located on the surface. Thus, the most reasonable mechanism is the following, with only the third species absorbing at 302 nm:



The data sets were fit simultaneously, using Dynafit [2], assuming $\epsilon_{302} = 10,400 \text{ M}^{-1}\text{cm}^{-1}$ for Ni(His₃Cys)NikR (this work). The model described above was used, with the following modification: the protein was assumed to be dimeric and to contain two sites, i.e. each Ni(II) is able to recognize two individual sites and bind accordingly. This was done in an attempt to take the tetrameric nature of NikR, with 4 HA sites, into account. Fitting using a model including all 4 sites requires simultaneous solution of 64 binding equilibria, which is too many for the Dynafit program. The validity of the simplification to assume dimeric NikR was confirmed by fitting using a more elaborate model assuming NikR is trimeric, and also assuming that NikR is tetrameric, but that it cannot bind more than two Ni(II) in the HA site at any given time. The results from these fitting procedures are essentially the same (as shown in Section V, see below), confirming that simplification of the binding model is permitted. Also, simulation using the resulting kinetic parameters of the degree of binding of the sites in NikR, assuming tetrameric NikR, indicated that the fraction of NikR containing more than two bound Ni(II) is negligible under the conditions of the experiments. The kinetic constants obtained from this fit correspond well to analytical fitting of the curves (see below). The reason that little effect is seen is probably that the excess of NikR over Ni(II) is over tenfold, and thus the 4 Ni(II) sites of each tetramer can be viewed individually.

The data were also fit analytically, using the following expression [3]:

$$y = \alpha \left[1 + \frac{\lambda_2}{\lambda_1 - \lambda_2} e^{-\lambda_1 t} - \frac{\lambda_1}{\lambda_1 - \lambda_2} e^{-\lambda_2 t} \right] \quad (6)$$

with α = amplitude, λ_1 = rate constant of the slow phase and λ_2 = rate constant of the fast phase, respectively. The dependent variable y is the baseline-corrected absorbance at 302 nm, which equates to the product ($[\text{Ni}(\text{His}_3\text{Cys})\text{NikR}] \cdot \epsilon_{302}$). This expression was used for non-linear regression, one curve at a time. For a two-step mechanism, the parameters λ_1 , λ_2 and α depend on the 4 rate constants of the reaction as follows [3]:

$$\lambda_1 = \frac{k_1 [\text{NikR}] (k_2 + k_{-2}) + k_{-1} k_{-2}}{k_1 [\text{NikR}] + k_{-1} + k_2 + k_{-2}} \quad (7)$$

$$\lambda_2 = k_1[NikR] + k_{-1} + k_2 + k_{-2} \quad (8)$$

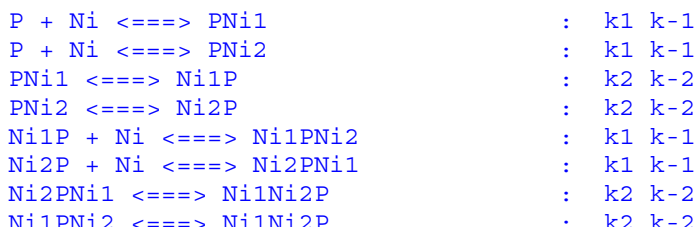
$$\alpha = \frac{K_1 K_2 [NikR]}{1 + K_1 [NikR] + K_1 K_2 [NikR]} \quad (9)$$

We found that the slow phase gave a hyperbolic dependence, whereas the fast phase showed too much scattering to be reasonably interpreted as a straight line. Direct fitting to eq. 7 yields $(k_2 + k_{-2}) = 0.1064$, in excellent agreement with the DynaFit results. At low $[NikR]$ ($<10 \mu\text{M}$), the linear dependence of the slow phase on $[NikR]$ has a slope $k_1(k_2 + k_{-2})/(k_{-1} + k_2 + k_{-2})$ and a y -axis cutoff $= k_{-1}k_{-2}/(k_{-1} + k_2 + k_{-2})$. Linear fitting at $[NikR] < 10 \mu\text{M}$ yields $k_1 = 16.9 (\pm 0.5) \text{ nM}^{-1}\text{s}^{-1}$ and $k_{-1}k_{-2}/(k_2 + k_{-2}) = 0.00513 (\pm 6.74 \cdot 10^{-4})$. This is in good agreement with the values expected from the DynaFit fits (which yields the calculated values 18.8 and 0.00598 for the slope and cutoff, respectively). Simulation of the hyperbolic curve with the values obtained from DynaFit also gave excellent results. Unfortunately, the hyperbolic curve cannot be fit independently, as the kinetic constants are too interdependent (as we cannot use extra information deriving from the fast phase, λ_2).

V. The applied Dynafit models

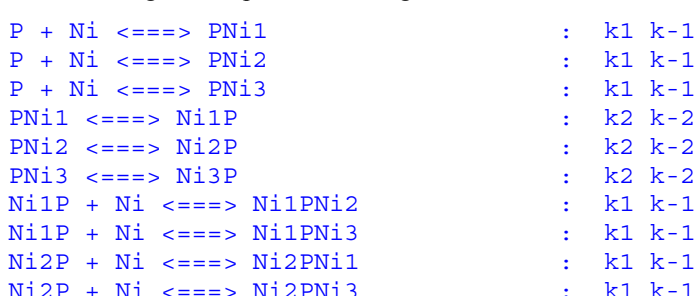
Model I: NikR as a dimer.

Each of both HA sites binds Ni(II) individually, through an intermediate. This results in 8 equilibria between 8 NikR species. The Ni(II) sites are named with arabic numerals. When the Ni(II) is bound to the (spectroscopically silent) intermediate, the letters Ni1 or Ni2 follow the letter P, and when bound to the final site, the letters Ni1 or Ni2 precede the letter P.

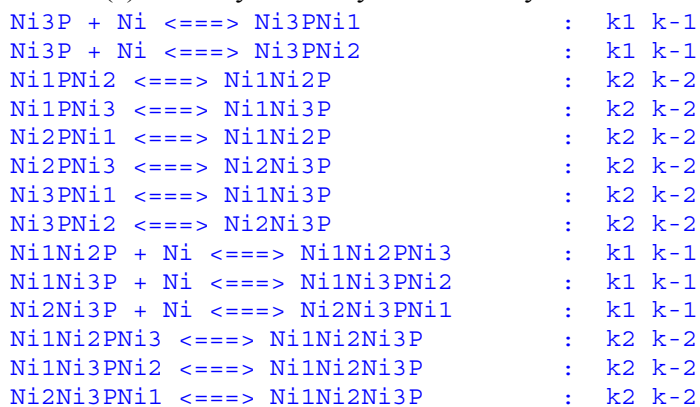


Model II: NikR as a trimer.

Each of the 3 HA sites binds Ni(II) individually, through an intermediate. This results in 24 equilibria between 20 NikR species. Naming of the species is analogous to above.

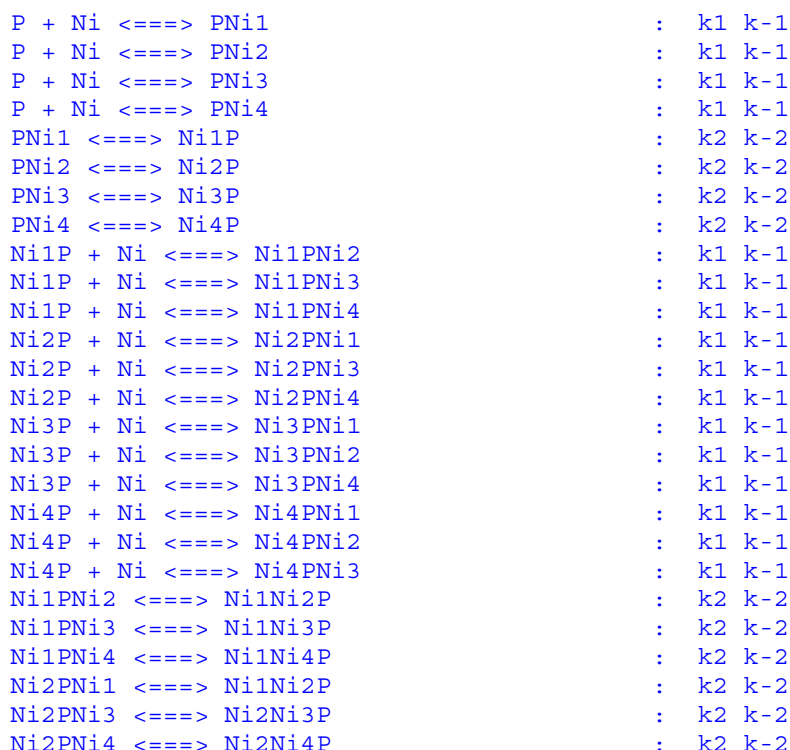


Supplementary Material (ESI) for Chemical Communications
 This journal is (c) The Royal Society of Chemistry 2008



Model III: NikR as a tetramer.

Each of the 4 HA sites binds Ni(II) individually, through an intermediate. This results in 64 equilibria between 48 NikR species. Naming of the species is analogous to above. Because the maximum number of equilibria allowed by the Dynafit fitting program is 50, it was necessary to simplify the mechanism. For this reason, the final 20 equilibria (indicated in red) were not used. The species involved in these equilibria contain three or more Ni(II) bound to the HA site, and are expected to be present at any given time in very low quantities under the conditions of the experiment (i.e. with an 10-fold excess or more of HA sites over Ni(II)). Simulations of the progress of the species with time, using the kinetic constants derived earlier are shown in Figure S2, below. Indeed, the percentage of signal at 302 nm derived from NikR containing only a single Ni(II) bound to the HA site is never lower than 85%, and the percentage of NikR tetramers containing more than two Ni(II) ions bound is negligible.



Supplementary Material (ESI) for Chemical Communications

This journal is (c) The Royal Society of Chemistry 2008

Ni ₃ PNi ₁	<====>	Ni ₁ Ni ₃ P	:	k ₂ k ₋₂
Ni ₃ PNi ₂	<====>	Ni ₂ Ni ₃ P	:	k ₂ k ₋₂
Ni ₃ PNi ₄	<====>	Ni ₃ Ni ₄ P	:	k ₂ k ₋₂
Ni ₄ PNi ₁	<====>	Ni ₁ Ni ₄ P	:	k ₂ k ₋₂
Ni ₄ PNi ₂	<====>	Ni ₂ Ni ₄ P	:	k ₂ k ₋₂
Ni ₄ PNi ₃	<====>	Ni ₃ Ni ₄ P	:	k ₂ k ₋₂
Ni ₁ Ni ₂ P + Ni	<====>	Ni ₁ Ni ₂ PNi ₃	:	k ₁ k ₋₁
Ni ₁ Ni ₂ P + Ni	<====>	Ni ₁ Ni ₂ PNi ₄	:	k ₁ k ₋₁
Ni ₁ Ni ₃ P + Ni	<====>	Ni ₁ Ni ₃ PNi ₂	:	k ₁ k ₋₁
Ni ₁ Ni ₃ P + Ni	<====>	Ni ₁ Ni ₃ PNi ₄	:	k ₁ k ₋₁
Ni ₁ Ni ₄ P + Ni	<====>	Ni ₁ Ni ₄ PNi ₂	:	k ₁ k ₋₁
Ni ₁ Ni ₄ P + Ni	<====>	Ni ₁ Ni ₄ PNi ₃	:	k ₁ k ₋₁
Ni ₂ Ni ₃ P + Ni	<====>	Ni ₂ Ni ₃ PNi ₁	:	k ₁ k ₋₁
Ni ₂ Ni ₃ P + Ni	<====>	Ni ₂ Ni ₃ PNi ₄	:	k ₁ k ₋₁
Ni ₂ Ni ₄ P + Ni	<====>	Ni ₂ Ni ₄ PNi ₁	:	k ₁ k ₋₁
Ni ₂ Ni ₄ P + Ni	<====>	Ni ₂ Ni ₄ PNi ₃	:	k ₁ k ₋₁
Ni ₃ Ni ₄ P + Ni	<====>	Ni ₃ Ni ₄ PNi ₁	:	k ₁ k ₋₁
Ni ₃ Ni ₄ P + Ni	<====>	Ni ₃ Ni ₄ PNi ₂	:	k ₁ k ₋₁
Ni ₁ Ni ₂ PNi ₃	<====>	Ni ₁ Ni ₂ Ni ₃ P	:	k ₂ k ₋₂
Ni ₁ Ni ₂ PNi ₄	<====>	Ni ₁ Ni ₂ Ni ₄ P	:	k ₂ k ₋₂
Ni ₁ Ni ₃ PNi ₂	<====>	Ni ₁ Ni ₂ Ni ₃ P	:	k ₂ k ₋₂
Ni ₁ Ni ₃ PNi ₄	<====>	Ni ₁ Ni ₃ Ni ₄ P	:	k ₂ k ₋₂
Ni ₁ Ni ₄ PNi ₂	<====>	Ni ₁ Ni ₂ Ni ₄ P	:	k ₂ k ₋₂
Ni ₁ Ni ₄ PNi ₃	<====>	Ni ₁ Ni ₃ Ni ₄ P	:	k ₂ k ₋₂
Ni ₂ Ni ₃ PNi ₁	<====>	Ni ₁ Ni ₂ Ni ₃ P	:	k ₂ k ₋₂
Ni ₂ Ni ₃ PNi ₄	<====>	Ni ₂ Ni ₃ Ni ₄ P	:	k ₂ k ₋₂
Ni ₂ Ni ₄ PNi ₁	<====>	Ni ₁ Ni ₂ Ni ₄ P	:	k ₂ k ₋₂
Ni ₂ Ni ₄ PNi ₃	<====>	Ni ₂ Ni ₃ Ni ₄ P	:	k ₂ k ₋₂
Ni ₃ Ni ₄ PNi ₁	<====>	Ni ₁ Ni ₃ Ni ₄ P	:	k ₂ k ₋₂
Ni ₃ Ni ₄ PNi ₂	<====>	Ni ₂ Ni ₃ Ni ₄ P	:	k ₂ k ₋₂
Ni ₁ Ni ₂ Ni ₃ P + Ni	<====>	Ni ₁ Ni ₂ Ni ₃ PNi ₄	:	k ₁ k ₋₁
Ni ₁ Ni ₂ Ni ₄ P + Ni	<====>	Ni ₁ Ni ₂ Ni ₄ PNi ₃	:	k ₁ k ₋₁
Ni ₁ Ni ₃ Ni ₄ P + Ni	<====>	Ni ₁ Ni ₃ Ni ₄ PNi ₂	:	k ₁ k ₋₁
Ni ₂ Ni ₃ Ni ₄ P + Ni	<====>	Ni ₂ Ni ₃ Ni ₄ PNi ₁	:	k ₁ k ₋₁
Ni ₁ Ni ₂ Ni ₃ PNi ₄	<====>	Ni ₁ Ni ₂ Ni ₃ Ni ₄ P	:	k ₂ k ₋₂
Ni ₁ Ni ₂ Ni ₄ PNi ₃	<====>	Ni ₁ Ni ₂ Ni ₃ Ni ₄ P	:	k ₂ k ₋₂
Ni ₁ Ni ₃ Ni ₄ PNi ₂	<====>	Ni ₁ Ni ₂ Ni ₃ Ni ₄ P	:	k ₂ k ₋₂
Ni ₂ Ni ₃ Ni ₄ PNi ₁	<====>	Ni ₁ Ni ₂ Ni ₃ Ni ₄ P	:	k ₂ k ₋₂

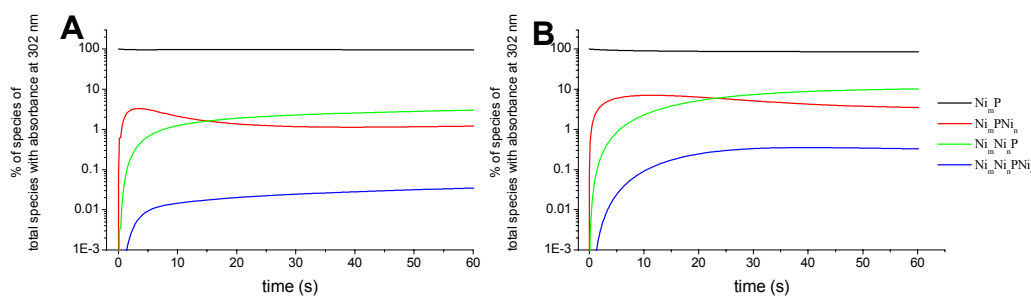


Figure S2. Percentage of Ni(II)-containing NikR species with at least one Ni(II) bound in the HA site, of the sum of all NikR species containing at least one Ni(II) in the HA site. The percentages result from simulations using the kinetic constants as described in the manuscript, using Model III. In A, the ratio Ni:NikR is 1:20 and in B, the ratio is 1:10.

Supplementary Material (ESI) for Chemical Communications

This journal is (c) The Royal Society of Chemistry 2008

The results of fitting of the data using these three models are shown in Table 1 below. The data that were fitted simultaneously are the five-trace averages of respective mixtures of Ni(II) and NikR in fixed ratios of 1:20 and 1:10, respectively, with Ni(II) varying from 0.2 to 64 μM ; and mixture with a fixed Ni(II) concentration of 6 μM , and NikR ranging from 10 to 105 μM .

Table 1

	$k_1 (10^4 \text{ M}^{-1}\text{s}^{-1})$	$k_{-1} (\text{s}^{-1})$	$k_2 (\text{s}^{-1})$	$k_{-2} (\text{s}^{-1})$
Model I	3.65 ± 0.46	0.095 ± 0.015	0.088 ± 0.016	0.0123 ± 0.0012
Model II	4.56 ± 0.94	0.091 ± 0.005	0.088 ± 0.011	0.0139 ± 0.0011
Model III	4.39 ± 0.42	0.110 ± 0.004	0.088 ± 0.002	0.0117 ± 0.0011
	$k_{\text{on}} (10^4 \text{ M}^{-1}\text{s}^{-1})$	$k_{\text{off}} (\text{s}^{-1})$	$K_D (\text{M})$	Sum of squares
Model I	1.76	0.0064	0.363	$1.11 \cdot 10^{-7}$
Model II	2.24	0.0071	0.316	$1.45 \cdot 10^{-7}$
Model III	2.24	0.0068	0.334	$1.98 \cdot 10^{-7}$

VI References

- (1) Fauquant C, Diederix REM, Rodrigue A, Dian C, Kapp U, Terradot L, Mandrand-Berthelot MA, Michaud-Soret I (2006) Biochimie 88: 1693-1705.
- (2) Kuzmic P (1996) Anal Biochem 237: 260-273.
- (3) Johnson KA (1986) Meth Enzymol 134: 677-705.
- (4) Halford SE (1975) Biochem J 149: 411-422.